

MITIGATING THE AUTOGENOUS SHRINKAGE OF ALKALI-ACTIVATED SLAG BY INTERNAL CURING

Zhenming Li (1), Mateusz Wyrzykowski (2), Hua Dong (1), Shizhe Zhang (1), Pietro Lura (2,3) and Guang Ye (1,4)

(1) Faculty of Civil Engineering and Geoscience, Delft University of Technology, the Netherlands

(2) Concrete/Construction Chemistry Laboratory, Empa, Swiss Federal Laboratories for Materials Science and Technology, Switzerland

(3) Institute for Building Materials, ETH Zurich, Switzerland

(4) Magnel Laboratory for Concrete Research, Department of Structural Engineering, Ghent University, Belgium

Abstract

Alkali activated slag (AAS) has shown promising potential to replace ordinary Portland cement as a binder material. Synthesized from industrial by-products, AAS can show high strength, thermal resistance and good durability. However, AAS has been reported to exhibit high autogenous shrinkage. Autogenous shrinkage is a critical issue for building materials since it can induce micro- or macro-cracking when the materials are under restrained conditions. Hence, this work aims at mitigating the autogenous shrinkage of AAS by means of internal curing. The influences of internal curing on microstructure formation and autogenous shrinkage are investigated. The results show that internal curing provided by superabsorbent polymers is a promising way to reduce the autogenous shrinkage of AAS.

Keywords: Internal curing, autogenous shrinkage, alkali-activated materials, slag, superabsorbent polymers (SAP)

1. INTRODUCTION

Alkali-activated slag (AAS) has emerged as an eco-friendly alternative to ordinary Portland cement (OPC) as a binder material. Compared with cement production, the production of AAS entails around 25-50% lower CO₂ emissions and more than 40% lower embodied energy [1,2]. AAS is typically prepared by mixing alkali solution with ground granulated blast-furnace slag (GGBFS), a by-product of the iron ore smelting industry [3]. When used as a binder material, AAS shows high strength, good chemical resistance and fire resistance [4–6]. However, several drawbacks of NaOH/Na₂SiO₃ activated slag, such as the fast setting and the large autogenous shrinkage, limit a wide application of this material in engineering practice. It has been reported in the literature that mixtures based on AAS can

exhibit several times higher autogenous shrinkage than mixtures based on OPC [7]. The high autogenous shrinkage of AAS can increase the risk of early-age cracking of the concrete [8].

Internal curing by SAP has been widely reported to have beneficial effects on mitigating the self-desiccation and the consequent autogenous shrinkage of Portland cement and blast-furnace slag cement pastes [9–14]. In AAS systems, the pore pressure resulting from self-desiccation is also an important driving force of autogenous shrinkage according to Collins and Sanjayan [15] and Ye and Radlińska [16]. Therefore, SAP should have potential in reducing the autogenous shrinkage of AAS. Despite this potential and the preliminary results reported in [17–20], studies in this field are still limited.

This study aims at exploring the effectiveness of internal curing by SAP in mitigating the autogenous shrinkage of NaOH/Na₂SiO₃ activated slag. The autogenous shrinkage of the plain and internally cured pastes were measured. X-ray computed tomography (CT) scan and scanning electron microscope (SEM) were utilized to observe the liquid desorption from the SAP and microstructure of the SAP-containing mixtures, respectively.

2. MATERIALS AND METHODS

2.1 Materials

The precursor used in this study was ground granulated blast-furnace slag (hereinafter termed slag) supplied by Ecocem Benelux. The chemical composition determined by X-ray fluorescence (XRF) is given in Table 1. The loss of ignition of the slag was determined according to ASTM D7348-08. The density of the slag is 2.89 g/cm³. The particle size range, determined by laser diffraction, was 0.1-50 μm, with a d₅₀ of 18.3 μm.

Table 1: Chemical compositions of slag

Oxide	SiO ₂	Al ₂ O ₃	CaO	MgO	Fe ₂ O ₃	TiO ₂	SO ₃	K ₂ O	MnO	Other
Slag	31.77	13.25	40.50	9.27	0.52	0.97	1.49	0.34	0.36	1.52

The alkaline activator was prepared by mixing anhydrous pellets of sodium hydroxide, deionized water and commercial sodium silicate solution (27.5 wt.% SiO₂, 8.25 wt.% Na₂O). The solution was then allowed to cool for 24 h before mixing with the precursor and dry SAP. The concentrations of Na₂O and SiO₂ in the activator were 9.5 wt.% (corresponding to 3.8 M) and 13.8 wt.%, respectively.

Solution-polymerized SAP of irregular particle shape and particle sizes of up to about 200 μm in the dry state were used.

2.2 Mixtures

The basic liquid/binder ratio (l/b) of the plain AAS paste is 0.5 (the control mixture). The absorption capacity of the SAP in the activator is 20g/g. The basic dosage of the SAP is 0.26%. The total l/b of AAS paste with SAP is therefore 0.552. Higher amounts of SAP (0.5% and 1%) and correspondingly higher amounts of internal curing activator are also applied (we assume that the SAP absorb the same amount, 20 g/g, of activator in mixtures with higher l/b). For each total l/b, a mixture without SAP is also set as reference. All mixtures compositions are shown in Table 2.

Table 2: Mixture compositions of AAS pastes with and without SAP (by mass proportion)

Mixture	AAS0.5	AAS0.55 2	AAS0.55 2SAP	AAS0.6	AAS0.6S AP	AAS0.7	AAS0.7S AP
Slag	1	1	1	1	1	1	1
Activator	0.5	0.552	0.552	0.6	0.6	0.7	0.7
SAP	-	-	0.0026	-	0.005	-	0.01

2.3 Measurement of initial and final set

The time of initial and final set was measured by an automatic Vicat setup with a measurement interval of 5 min. The samples were covered with a plastic film during the measurement in order to limit the evaporation from the surface [12].

2.4 Linear autogenous shrinkage

The linear autogenous shrinkage of the pastes was measured by the corrugated tube method [21], in which three sealed corrugated tubes about 425 mm long and Ø 28.5 mm were used for each mixture. After mixing, the fresh paste was carefully cast into the corrugated tubes and sealed by plugs. The length changes were automatically measured on three specimens in parallel placed on a stainless-steel bench (immersed in a temperature-controlled silicone-oil bath) by linear variable differential transformers (LVDTs) until 7 days. A detailed description of the method can be found in [22]. The strains are referenced to the length of the sample at the time of final set determined by Vicat needle on the corresponding paste in parallel tests, where the samples were protected from evaporation by means of a plastic film. The automatic measurements show a low scatter for triplicate samples, with the relative standard error in the range of 1–2% after the final set of the materials.

2.5 X-ray microcomputed tomography

To study the absorption and desorption behavior of SAP in AAS paste, the mixture AAS0.552SAP was scanned using CT scan through a Phoenix Nanotom CT scanner. The paste was first cast into a small plastic container with a diameter of 4 mm and a height of 6 mm. Immediately after casting, the container was sealed by paraffin film and put into the CT scanner. During the first week after casting, the same sample was scanned at the age of 1 hour, 8 hours, 1 day and 7 days, respectively. The duration of each scan was one hour. The spatial resolution was 5 µm. 3D Reconstruction was carried out with VG Studio Max.

2.6 SEM analysis

The fracture surface of internally cured paste and the voids left by the SAP were observed using SEM. The paste AAS0.552SAP was cast into a PVC cylinder bottle with a diameter of 24 mm and a height of 50 mm. At the age of 7 days, the sample was taken out from the bottle and crushed into pieces with a size of around 1 cm³. These pieces were then immersed in isopropanol for a week to stop the reaction. During that period, the isopropanol was replaced every two days. Afterwards, the samples were put into a moderate vacuum as obtained by an aspirator pump until a constant weight (<0.1%) was obtained. After carbon coating, the

samples were imaged with an environmental scanning electron microscope (Philips- XL30-ESEM) in secondary electron mode in high vacuum.

3. RESULTS AND DISCUSSION

3.1 Setting time

The times of initial and final set are shown in Table 3. The initial and final set occur later for pastes with higher l/b without SAP. However, for pastes with SAP, the time of initial set is similar to that of the control mixture AAS0.5, which is likely due to the similar basic l/b of these mixtures. The times of final set of SAP-containing pastes are longer than for the control mixture but shorter than for the non-SAP mixtures with the same total l/b.

Table 3: Times of initial and final set for AAS pastes with and without SAP

Mixture	AAS0.5	AAS0.5 52	AAS0.5 52SAP	AAS0.6	AAS0.6 SAP	AAS0.7	AAS0.7 SAP
Initial set (min)	25	36	24	40	25	55	35
Final set (min)	35	51	39	65	56	80	70

3.2 Autogenous shrinkage

Figure 1 shows the linear autogenous shrinkage of the plain and internally cured AAS pastes in the first week of reaction. It can be seen that the shrinkage of the control mixture AAS0.5 develops rapidly after setting, reaching 3630 $\mu\text{m}/\text{m}$ at 1 day and around 6600 $\mu\text{m}/\text{m}$ at 7 days. Increasing the liquid content without adding SAP reduces the autogenous shrinkage slightly. By adding 0.26 wt. % SAP, the autogenous shrinkage is dramatically reduced. Increasing the SAP dosage (together with the corresponding absorbed liquid amount) to 0.5% or 1% does not lead to any significant change in the measured shrinkage.

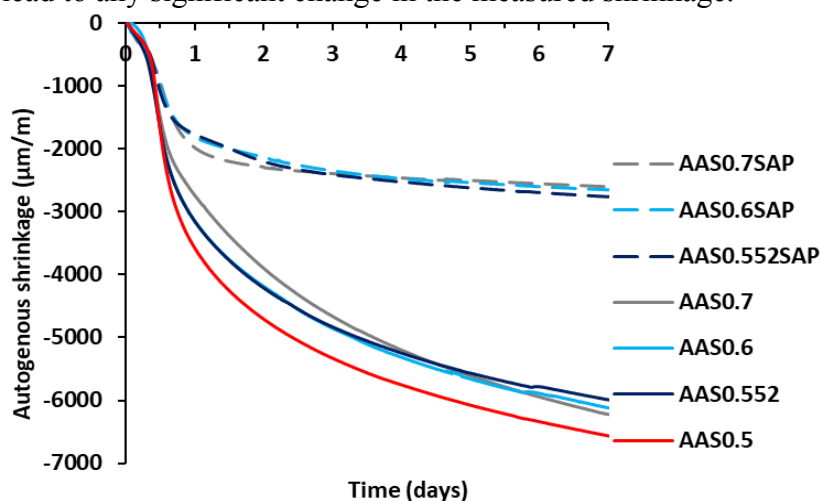


Figure 1: Autogenous shrinkage of AAS pastes with different l/b and different amounts of SAP. Each curve shows the average result of three samples.

3.3 X-ray micro-computed tomography analysis

The evolution of a horizontal cross-section of AAS0.552SAP obtained from the CT scan is shown in Figure 2. Based on the grey levels, several phases can be distinguished within the paste, including unreacted slag particles (white), SAP with liquid (dark grey), entrapped air (black and spherical) and newly formed voids/pores (black, marked by the arrows) within the SAP-originated voids.

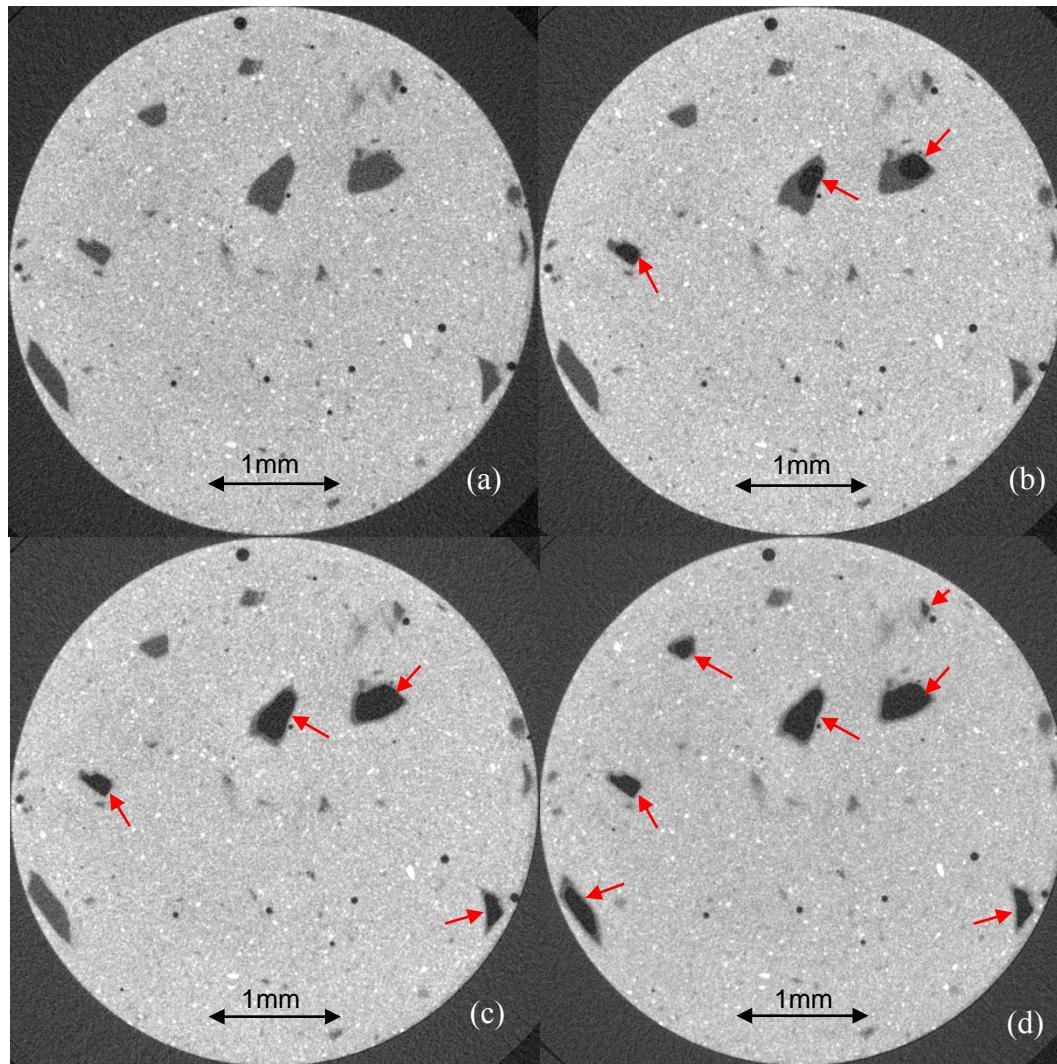


Figure 2: A representative cross-section of AAS0.552SAP paste obtained by X-ray microtomography at the curing age of (a) 1 hour, (b) 8 hours, (c) 1 day and (d) 7 days.

Figure 2 (a) shows the randomly distributed swollen SAP particles in the paste, indicating a successful absorption of liquid by SAP. The size of SAP in the paste can reach more than 0.5 mm. At the age of 8 h (Figure 2 (b)), air voids have already formed within the voids originally occupied by the swollen SAP, indicating the liquid release from SAP to the surrounding paste, i.e. internal curing. At the age of 1 day, the area of newly formed voids increases, indicating more liquid is released from the SAP. At the age of 7 days, most of the

SAP particles located at the chosen cross-section have been emptied, but some of them still have liquid stored inside, which could be distinguished by the dark grey colour of these SAP-originated voids. This part of liquid can be useful to compensate the self-desiccation occurring after 7 days. At the given resolution, no reaction products forming inside the SAP voids could be identified.

Figure 3 (a) and 3 (b) show two representative SEM images of the microstructure of AAS0.552SAP paste cured for 7 days. Figure 3 (c) shows a representative interface between SAP and the surrounding paste. From the images, the dry SAP and the surrounding paste can be clearly distinguished based on their surface features: SAP have a locally porous microstructure while the paste is dense and homogenous. The SAP particle shown in Figure 3 (a) has a big void inside, with a smooth curved surface, which is consistent with the CT scan observations in Figure 2. Figure 3 (b) shows a void that is filled with SAP. This can be due to either that the liquid inside the SAP particle has not been consumed yet at the moment of hydration stoppage or that the liquid has been consumed but the dry SAP particle left agglomerates into the void shown in Figure 3 (b). In both Figure 3 (a) and (b), a rim of paste can be observed surrounding the SAP particle, with a relatively smoother surface and fewer unreacted slag particles embedded. This could be due to the liquid released from the SAP particle resulting in a local increase of l/b in the rim.

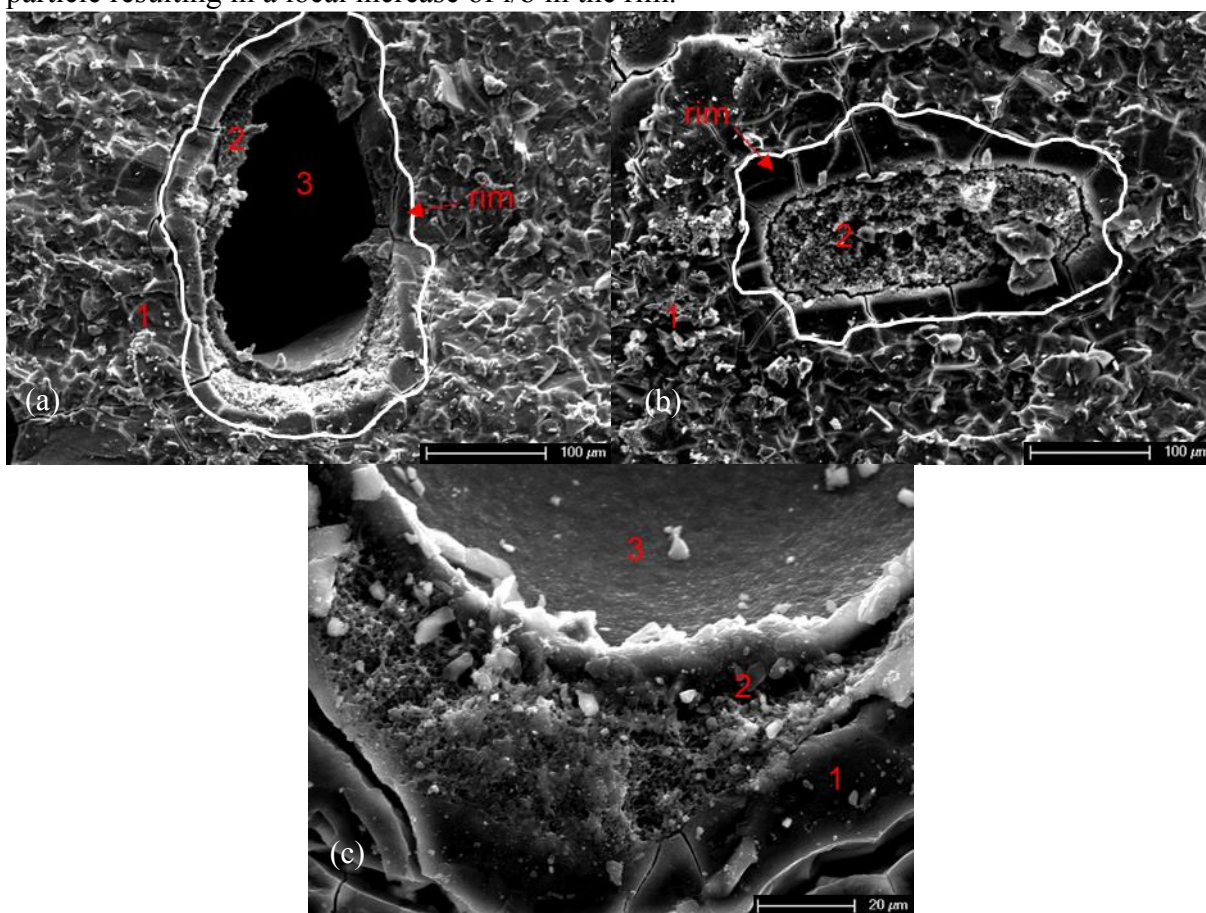


Figure 3: SEM images of the SAP-originated voids in paste AAS0.552SAP cured for 7 days. (a) and (b) shows a void that is partly and fully filled by dry SAP, respectively. (c)

shows an interface between SAP and surrounding paste. 1 indicates the paste, 2 indicates the dry SAP and 3 indicates the SAP-originated voids

4. CONCLUSIONS

Based on the results and discussion, the following conclusions can be drawn:

- Internal curing by SAP delays the times of initial and final set.
- Internal curing by SAP can largely mitigate the autogenous shrinkage of NaOH/Na₂SiO₃ activated slag. This is beneficial for tackling the problem of large autogenous shrinkage of AAS in practical applications. Larger amounts of SAP than 0.26 wt.% do not bring further mitigation of autogenous shrinkage of the AAS paste studied.
- In the internally cured sample, the SAP are observed to release liquid to the surrounding paste starting from before 8 h. After the first week, there is still a certain amount of liquid left in SAP for mixture AAS0.552SAP, indicating a further internal curing potential for later reactions.

ACKNOWLEDGEMENTS

This work is supported in part by the scholarship from China Scholarship Council (CSC) and the grant from the Netherlands Organisation for Scientific Research (NWO). The short visit at Empa by the first author was supported by STSM project from COST Action TU1404 “Towards the next generation of standards for the service life of cement-based materials and structures”

REFERENCES

- [1] R.J. Thomas, H. Ye, A. Radlinska, S. Peethamparan, Alkali-activated slag cement concrete, *Concr. Int.* 38 (2016) 33–38.
- [2] P. Duxson, J.L. Provis, G.C. Lukey, J.S.J. van Deventer, The role of inorganic polymer technology in the development of “green concrete,” *Cem. Concr. Res.* 37 (2007) 1590–1597. doi:10.1016/j.cemconres.2007.08.018.
- [3] C. Shi, A.F. Jiménez, A. Palomo, New cements for the 21st century: The pursuit of an alternative to Portland cement, *Cem. Concr. Res.* 41 (2011) 750–763. doi:10.1016/j.cemconres.2011.03.016.
- [4] J.L. Provis, J.S.J. Van Deventer, *Geopolymers: structures, processing, properties and industrial applications*, Woodhead, Cambridge, UK, 2009.
- [5] K. Arbi, M. Nedeljković, Y. Zuo, G. Ye, A Review on the Durability of Alkali-Activated Fly Ash/Slag Systems: Advances, Issues, and Perspectives, *Ind. Eng. Chem. Res.* 55 (2016) 5439–5453. doi:10.1021/acs.iecr.6b00559.
- [6] M.C.G. Juenger, F. Winnefeld, J.L. Provis, J.H. Ideker, Advances in alternative cementitious binders, *Cem. Concr. Res.* 41 (2011) 1232–1243. doi:10.1016/j.cemconres.2010.11.012.
- [7] Z. Li, M. Nedeljkovic, Y. Zuo, G. Ye, Autogenous shrinkage of alkali-activated slag-fly ash pastes, in: *5th Int. Slag Valor. Symp.*, Leuven, 2017: pp. 369–372.
- [8] Z. Li, A. Kostiuchenko, G. Ye, Autogenous shrinkage-induced stress of alkali-activated slag and fly ash concrete under restraint condition, in: *ECI (Ed.), Alkali Act. Mater. Geopolymers Versatile Mater. Offer. High Perform. Low Emiss.*, Tomar, 2018: p. 24.

- [9] V. Mechtcherine, M. Gorges, C. Schroefl, A. Assmann, W. Brameshuber, A.B. Ribeiro, D. Cusson, J. Custódio, E.F. Da Silva, K. Ichimiya, S.I. Igarashi, A. Klemm, K. Kovler, A.N. De Mendonça Lopes, P. Lura, V.T. Nguyen, H.W. Reinhardt, R.D.T. Filho, J. Weiss, M. Wyrzykowski, G. Ye, S. Zhutovsky, Effect of internal curing by using superabsorbent polymers (SAP) on autogenous shrinkage and other properties of a high-performance fine-grained concrete: Results of a RILEM round-robin test, *Mater. Struct. Constr.* 47 (2014) 541–562. doi:10.1617/s11527-013-0078-5.
- [10] O.M. Jensen, P.F. Hansen, Water-entrained cement-based materials - I. Principles and theoretical background, *Cem. Concr. Res.* 31 (2001) 647–654. doi:10.1016/S0008-8846(01)00463-X.
- [11] P. Lura, F. Durand, O.M. Jensen, Autogenous strain of cement pastes with superabsorbent polymers, *Proc. International RILEM Conf. Vol. Chang. Hardening Concr. Test. Mitig. C* (2006) 57–66. doi:10.1617/2351580052.007.
- [12] J. Justs, M. Wyrzykowski, D. Bajare, P. Lura, Internal curing by superabsorbent polymers in ultra-high performance concrete, *Cem. Concr. Res.* 76 (2015) 82–90. doi:10.1016/j.cemconres.2015.05.005.
- [13] D. Snoeck, O.M. Jensen, N. De Belie, The influence of superabsorbent polymers on the autogenous shrinkage properties of cement pastes with supplementary cementitious materials, *Cem. Concr. Res.* 74 (2015) 59–67. doi:10.1016/j.cemconres.2015.03.020.
- [14] M. Wyrzykowski, P. Lura, Reduction of autogenous shrinkage in OPC and BFSC pastes with internal curing, in: *Proc. XIII Int. Conf. Durab. Build. Mater. Components*, São Paulo, Brazil, 2014: pp. 2–5.
- [15] F. Collins, J. Sanjayan, Effect of pore size distribution on drying shrinking of alkali-activated slag concrete, *Cem. Concr. Res.* 30 (2000) 1401–1406. doi:10.1016/S0008-8846(00)00327-6.
- [16] H. Ye, A. Radlińska, Shrinkage mechanisms of alkali-activated slag, *Cem. Concr. Res.* 88 (2016) 126–135. doi:10.1016/j.cemconres.2016.07.001.
- [17] A.R. Sakulich, D.P. Bentz, Mitigation of autogenous shrinkage in alkali activated slag mortars by internal curing, *Mater. Struct.* 46 (2013) 1355–1367. doi:10.1617/s11527-012-9978-z.
- [18] S. Oh, Y.C. Choi, Superabsorbent polymers as internal curing agents in alkali activated slag mortars, *Constr. Build. Mater.* 159 (2018) 1–8. doi:10.1016/j.conbuildmat.2017.10.121.
- [19] C. Song, Y.C. Choi, S. Choi, Effect of internal curing by superabsorbent polymers – Internal relative humidity and autogenous shrinkage of alkali-activated slag mortars, *Constr. Build. Mater.* 123 (2016) 198–206. doi:10.1016/j.conbuildmat.2016.07.007.
- [20] W. Tu, Y. Zhu, G. Fang, X. Wang, M. Zhang, Internal curing of alkali-activated fly ash-slag pastes using superabsorbent polymer, *Cem. Concr. Res.* 116 (2019) 179–190. doi:10.1016/j.cemconres.2018.11.018.
- [21] ASTM C1968, Standard Test Method for Autogenous Strain of Cement Paste and Mortar, (2013) 1–8. doi:10.1520/C1698-09.2.
- [22] M. Wyrzykowski, Z. Hu, S. Ghourchian, K. Scrivener, P. Lura, Corrugated tube protocol for autogenous shrinkage measurements: review and statistical assessment, *Mater. Struct.* 50 (2017) 57. doi:10.1617/s11527-016-0933-2.